Electronic Supplementary Information

In-situ structural evolution of multi-site alloy electrocatalyst to manipulate intermediate for enhanced water oxidation reaction

Bingliang Wang,[a] Kangning Zhao,[b] Zhuo Yu,[a] Congli Sun,[b,c] Zhuo Wang,[a] Ningning Feng,[a] Liqiang Mai,[b] Yonggang Wang, *[a] Yongyao Xia*[a]

Affiliations:

a. Department of Chemistry and Shanghai Key Laboratory of Molecular Catalysis and Innovative Materials, Institute of New Energy, iChEM (Collaborative Innovation Center of Chemistry for Energy Materials) Fudan University, Shanghai 200433, China.
b. State Key Laboratory of Advanced Technology for Materials Synthesis and Processing, State Key Laboratory of Silicate Materials for Architectures, International School of Materials Science and Engineering, Wuhan University of Technology, Wuhan 430070, P. R. China.
c. NRC (Nanostructure Research Centre), Wuhan University of Technology, Wuhan 430070, P. R. China.

* E-mail: ygwang@fudan.edu.cn , yyxia@fudan.edu.cn

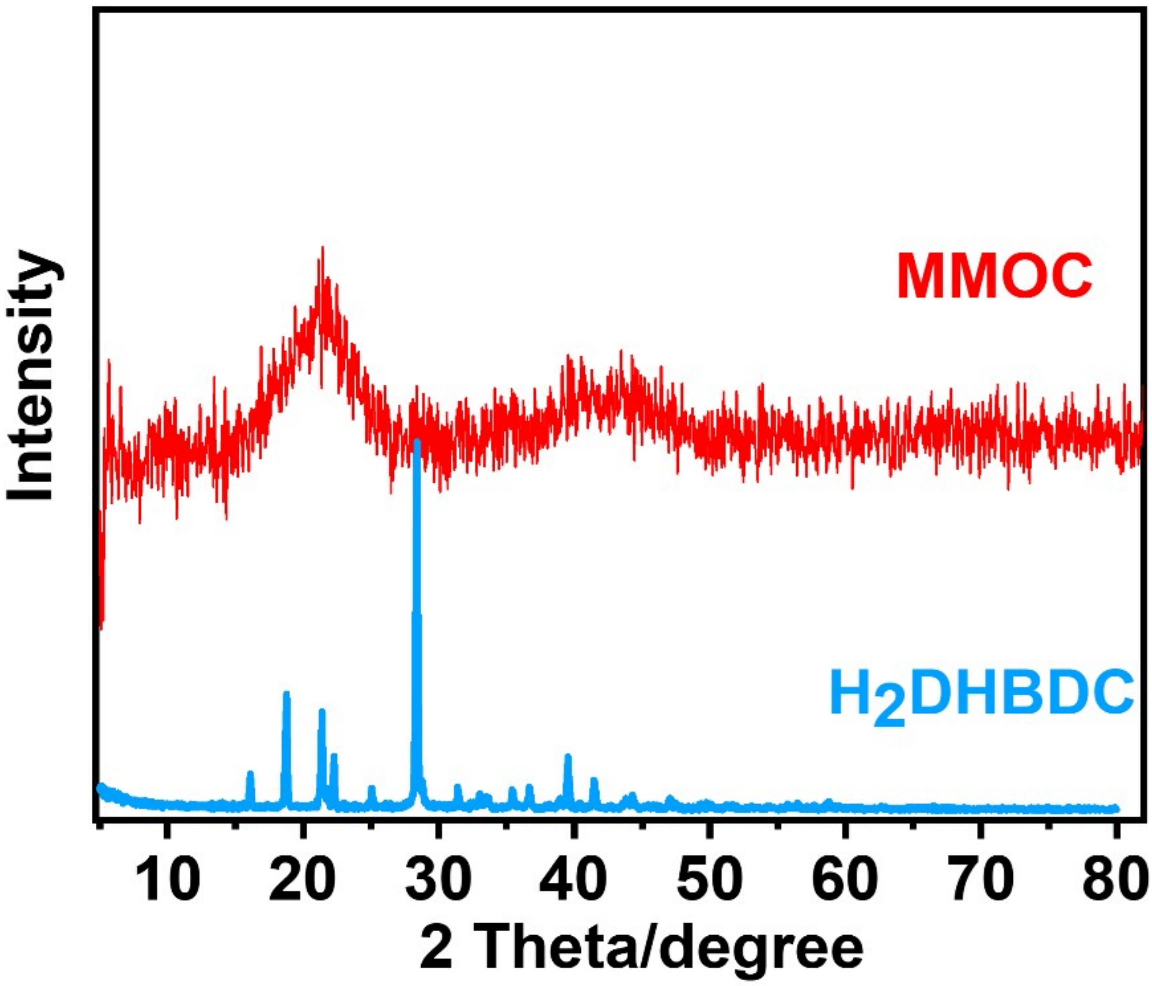

Fig. S1，The XRD pattern of MMOC.

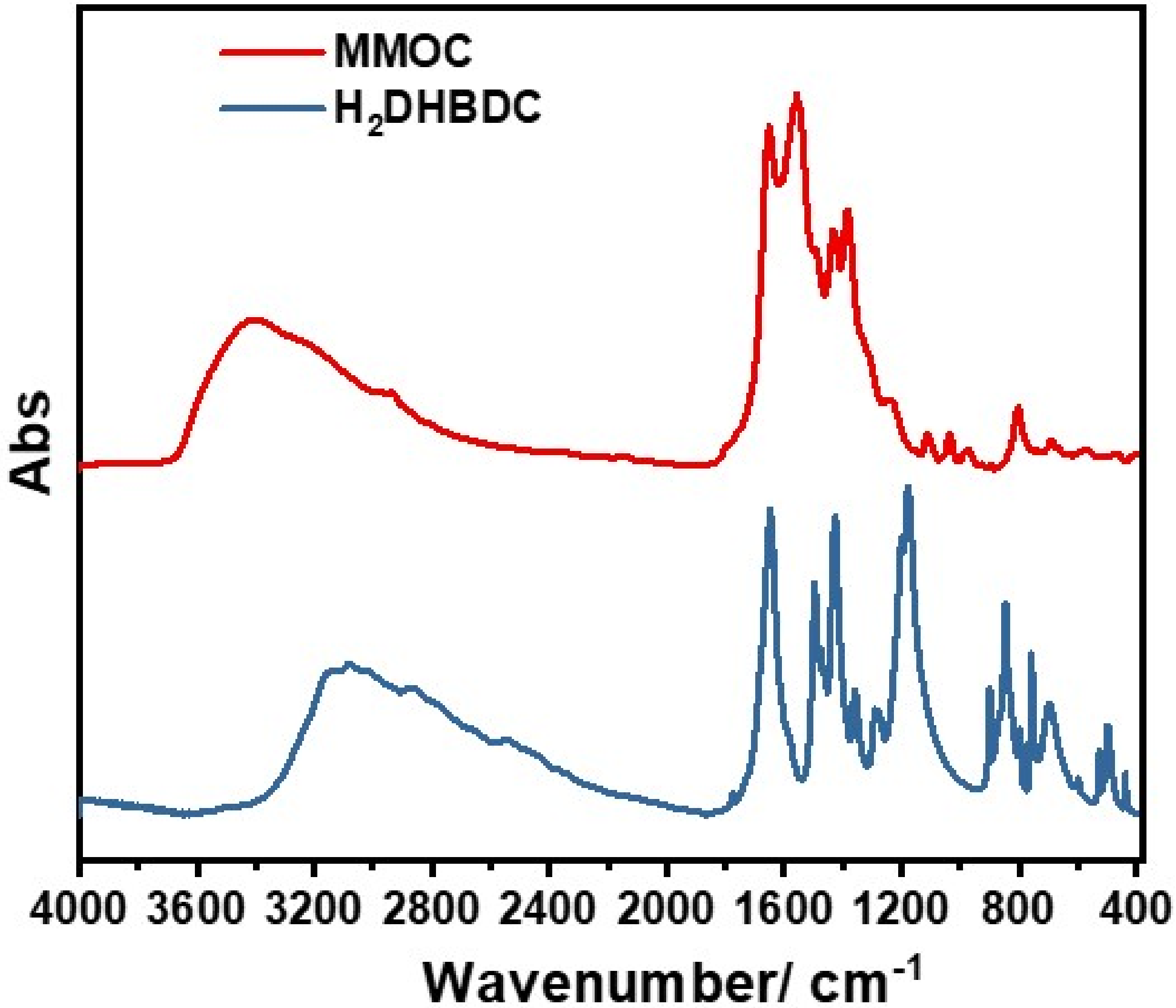

Fig. S2, FT-IR spectrum of MMOC and H_2DHBDC ligand.

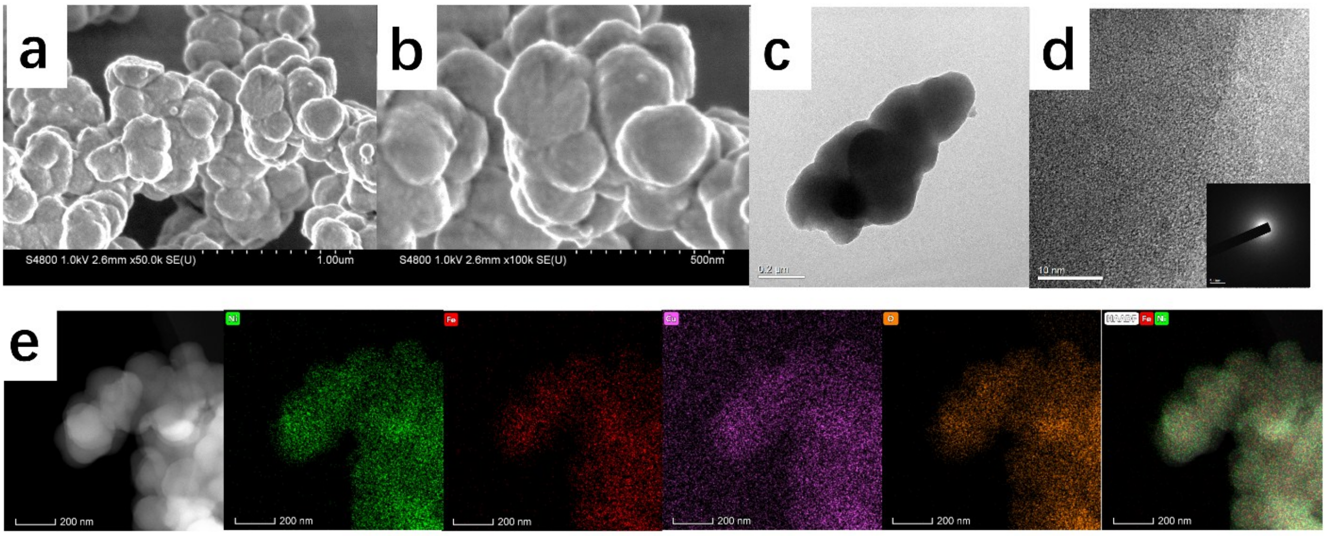

Fig. S3. (a-b) SEM images of MMOC. (c) TEM image of MMOC. (d)HRTEM image of MMOC,Inset image:corresponding SAED pattern.(e) HAADF-STEM images and corresponding EDS mapping analysis of MMOC. Scale bar: (a) 1 µm, (b) 500 nm, (c) 200 nm , (d) 10 nm inset image: 5 1/nm and (e) 200 nm

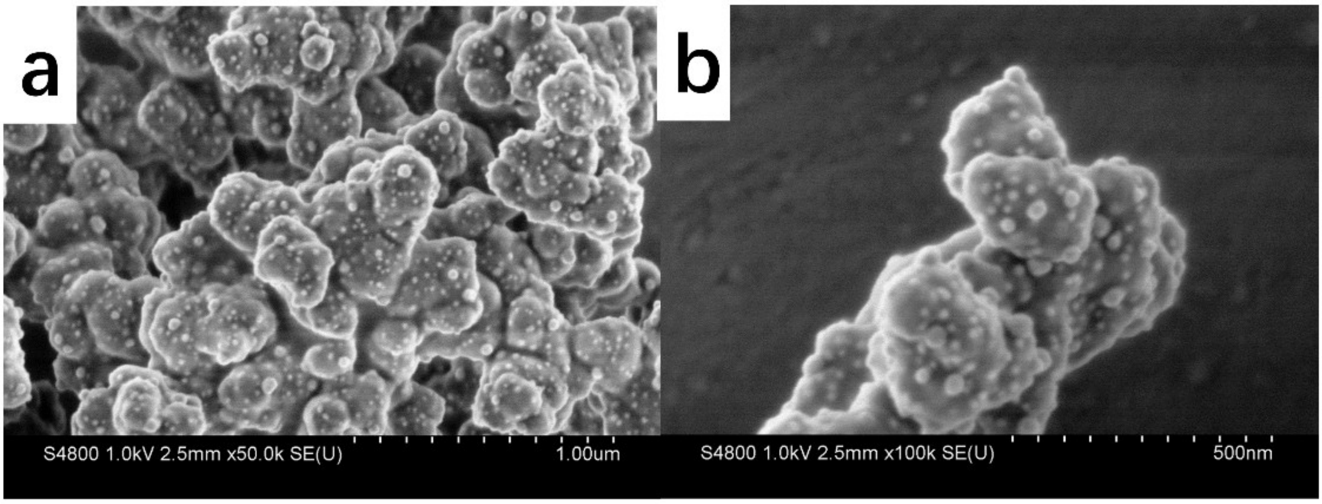

Fig. S4. SEM images of MsA. Scale bar: (a) 1 μm and (b) 500 nm.

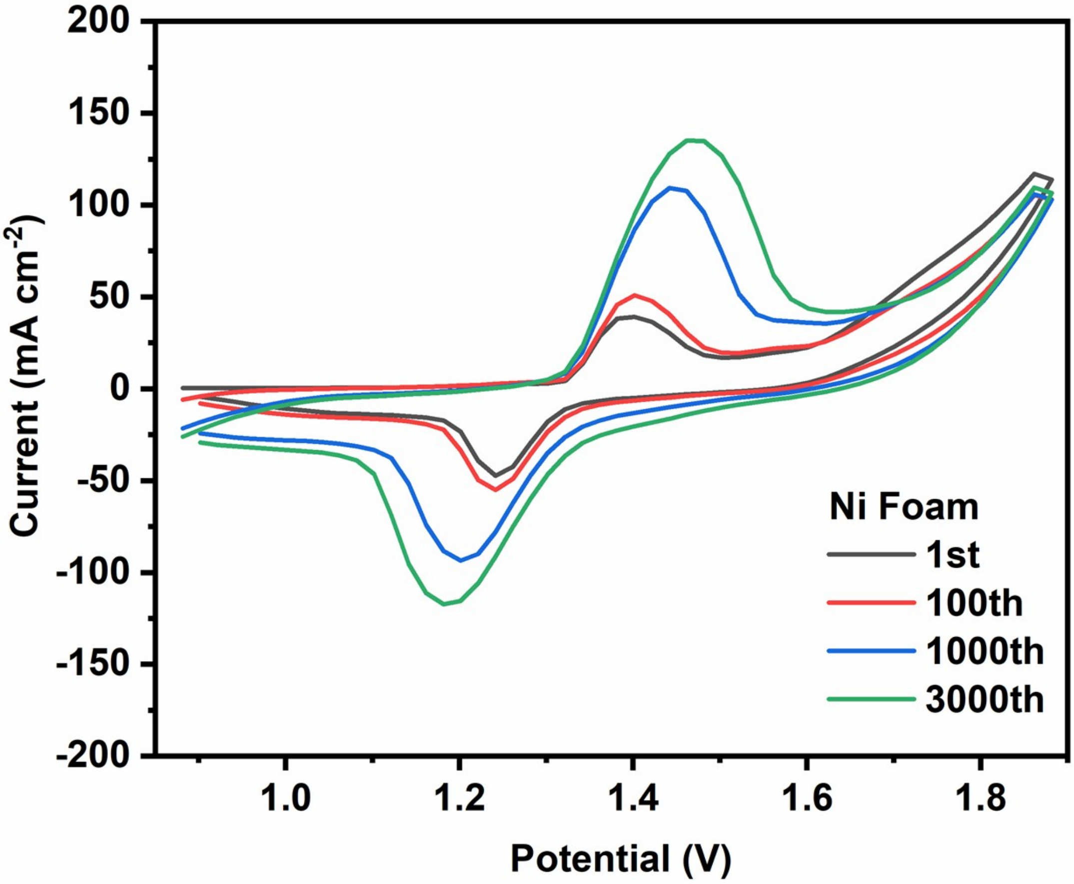

Fig. S5. CV curves of electrochemical dealloying process for Ni foam. (Cycle 1, 100, 1000 and 3000 were selected, all CV curves without iR-correction) scan rate:100 mV s^{-1}.

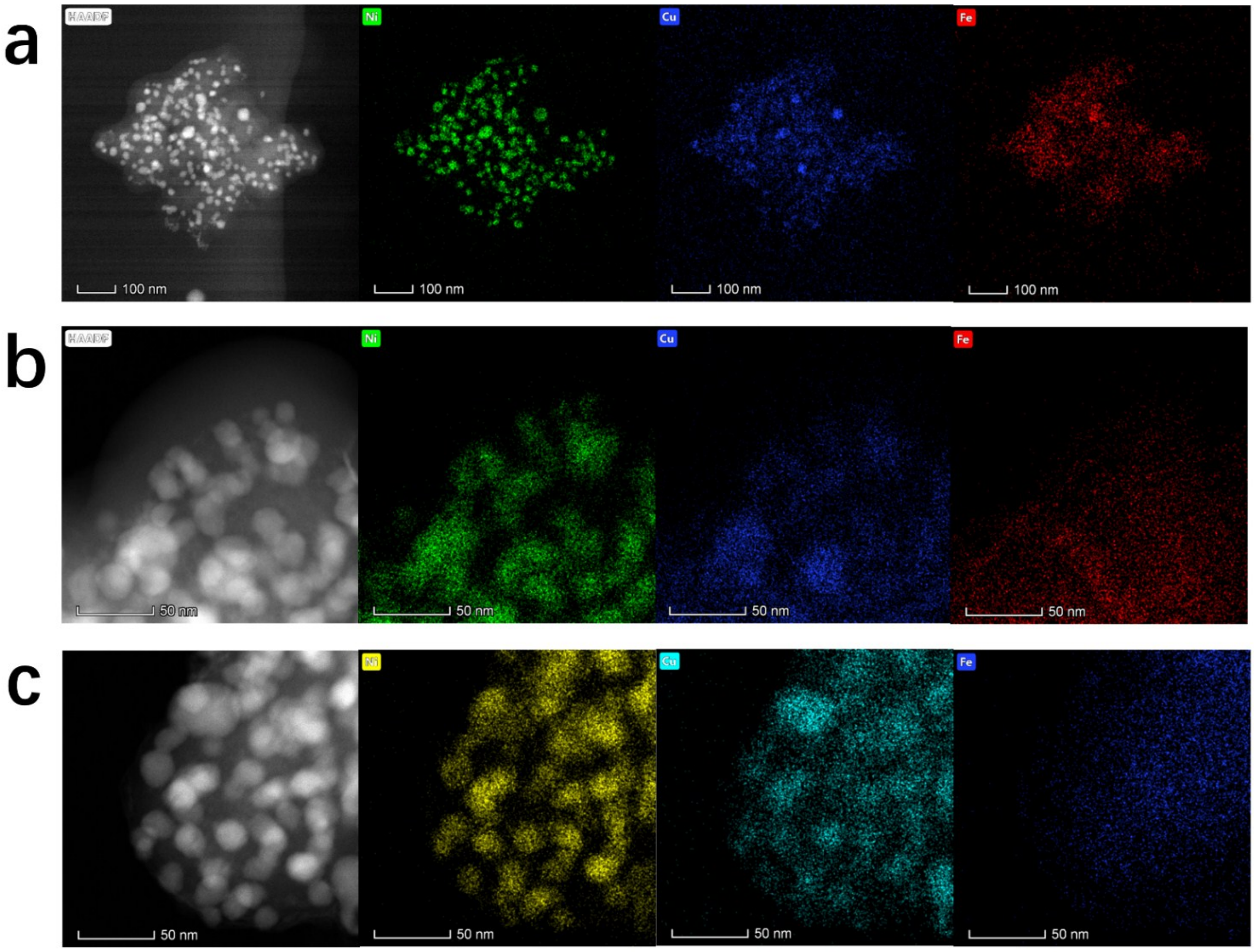

Fig. S6. HAADF-STEM images and corresponding EDS elemental mapping analysis of (a) 1 st CV (b) 100 th CV (c) 1000th CV. Scale bar: (a) 100 nm ,(b) 50 nm and (c) 50 nm.

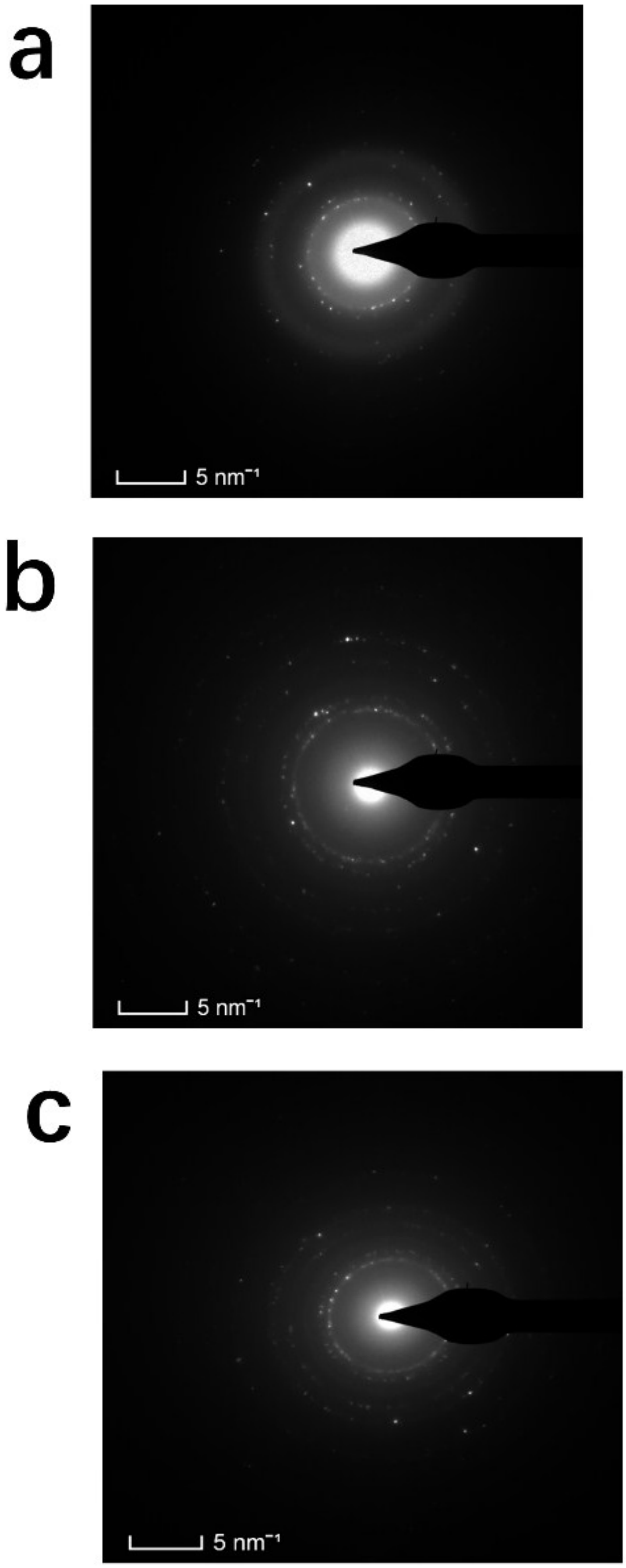

Fig. S7. SAED pattern of (a) 1 st CV (b) 100 th CV (c) 1000th CV. Scale bar : 5 nm^{-1}

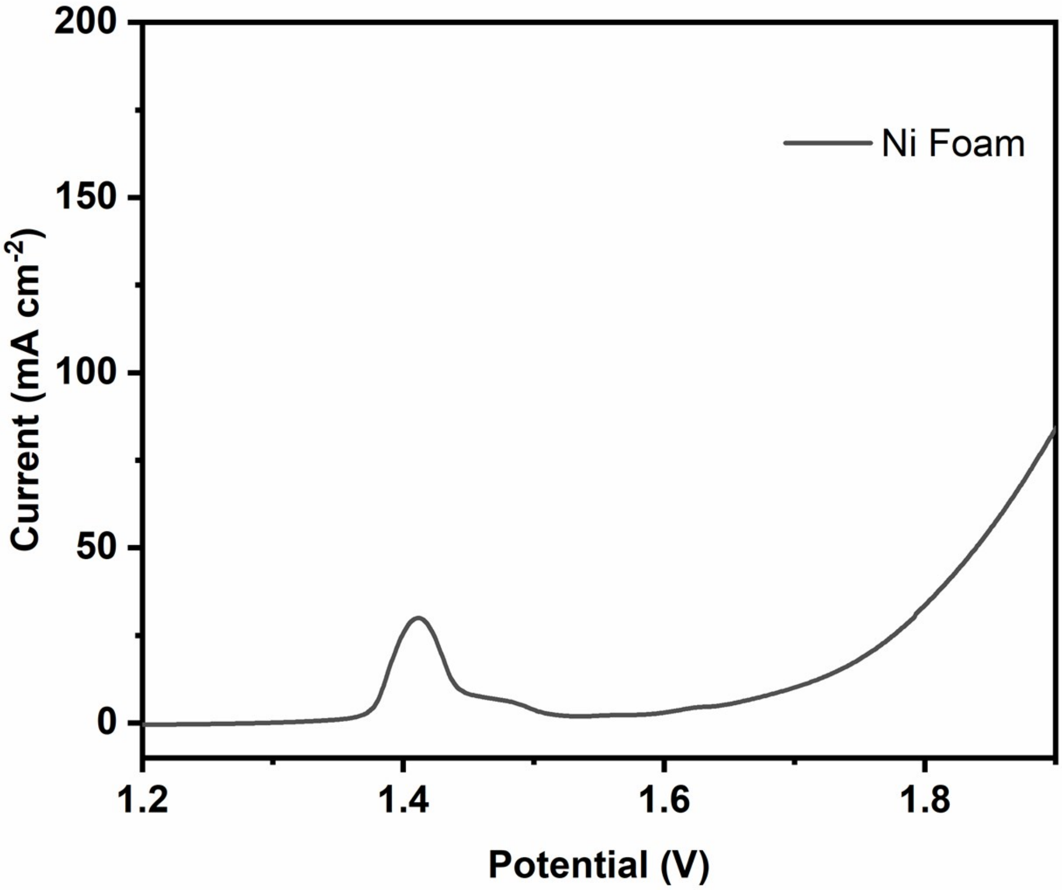

Fig. S8. LSV curve of Ni foam after 3000 cycles. Scan rate: 5 mV s^{-1}.

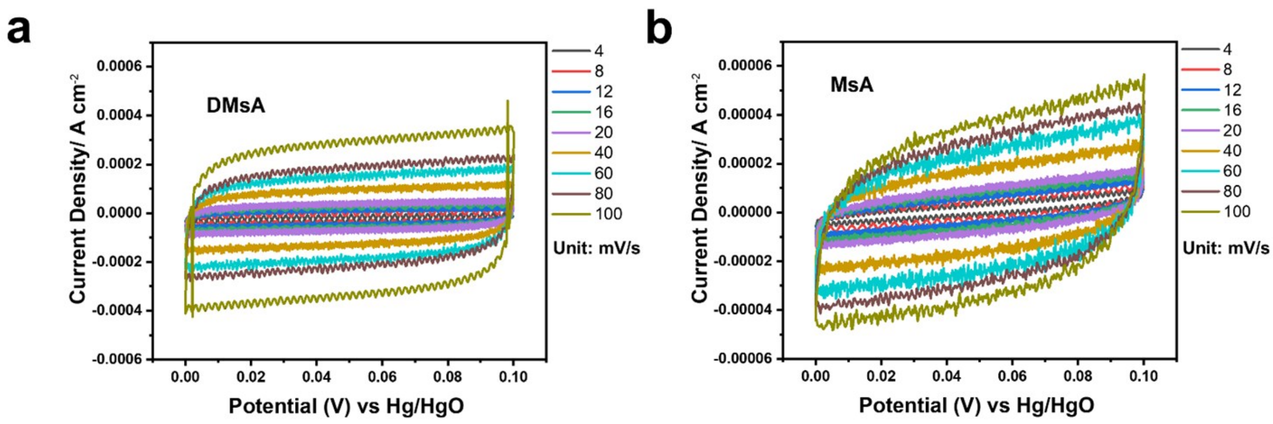

Fig. S9. CV tests at various scan rates for calculating the ECSA.

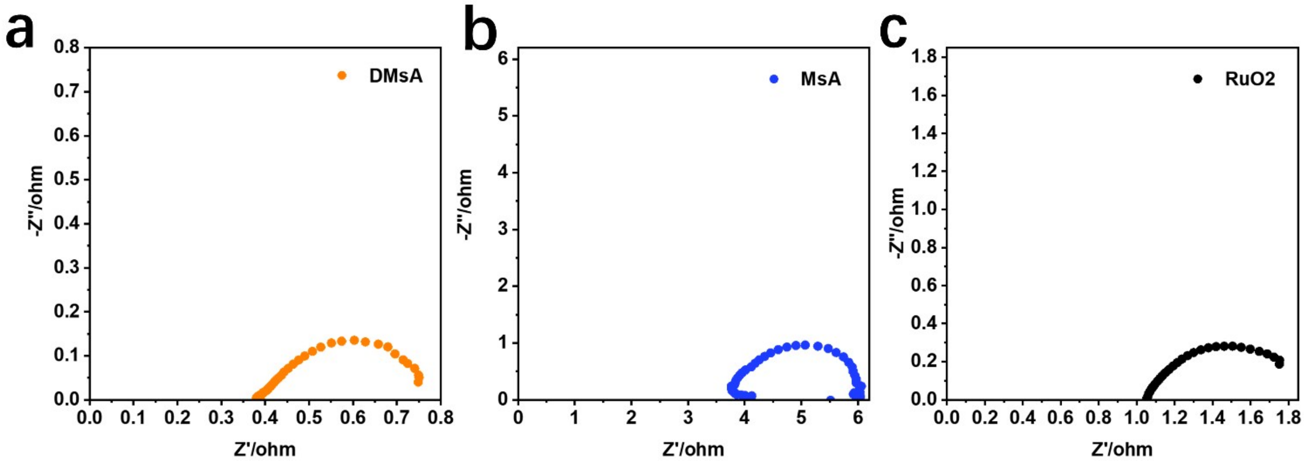

Fig. S10. EIS analysis performed at the potential corresponding with 100 mA cm^{-2} of LSV curves. (a) DMsA, (b) MsA and (c) commerical RuO_2 catalyst.

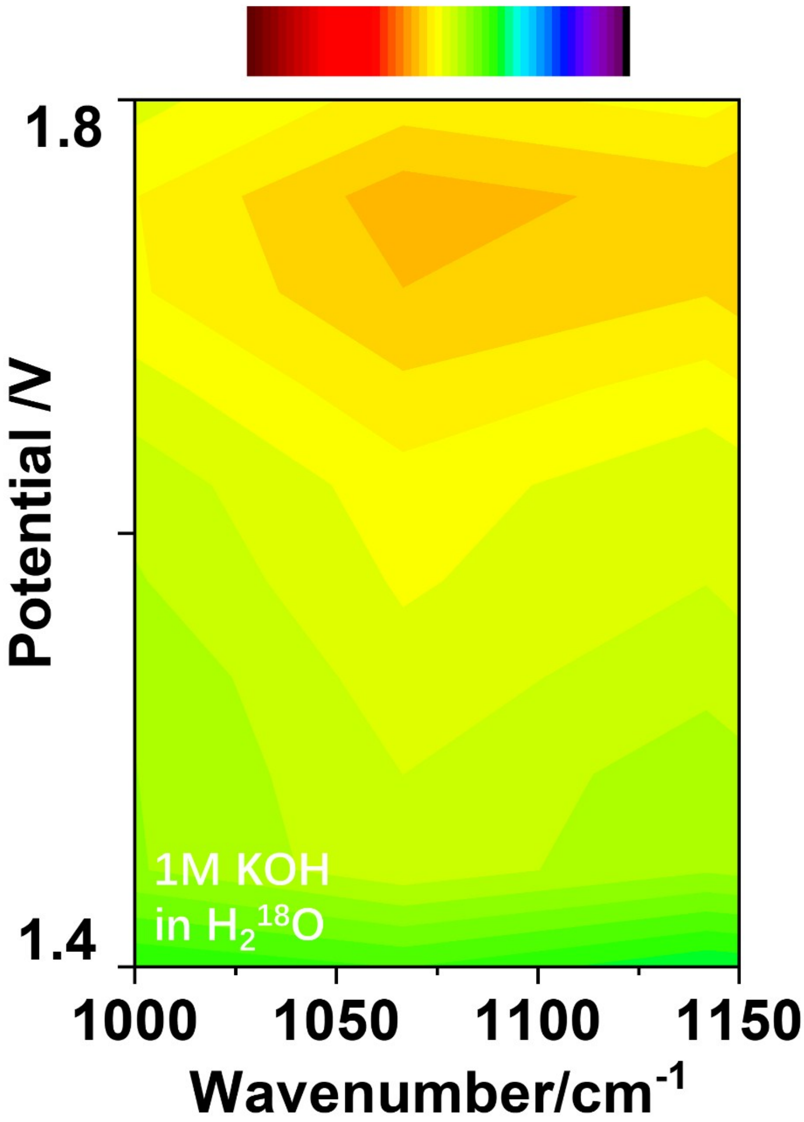

Fig. S11. 2D contour image of operando ATR FT-IR spectrum for DMsA electrocatalyst in 1 M KOH in $H_2{}^{18}O$ at the potential range from 1.4 to 1.8 V vs RHE.

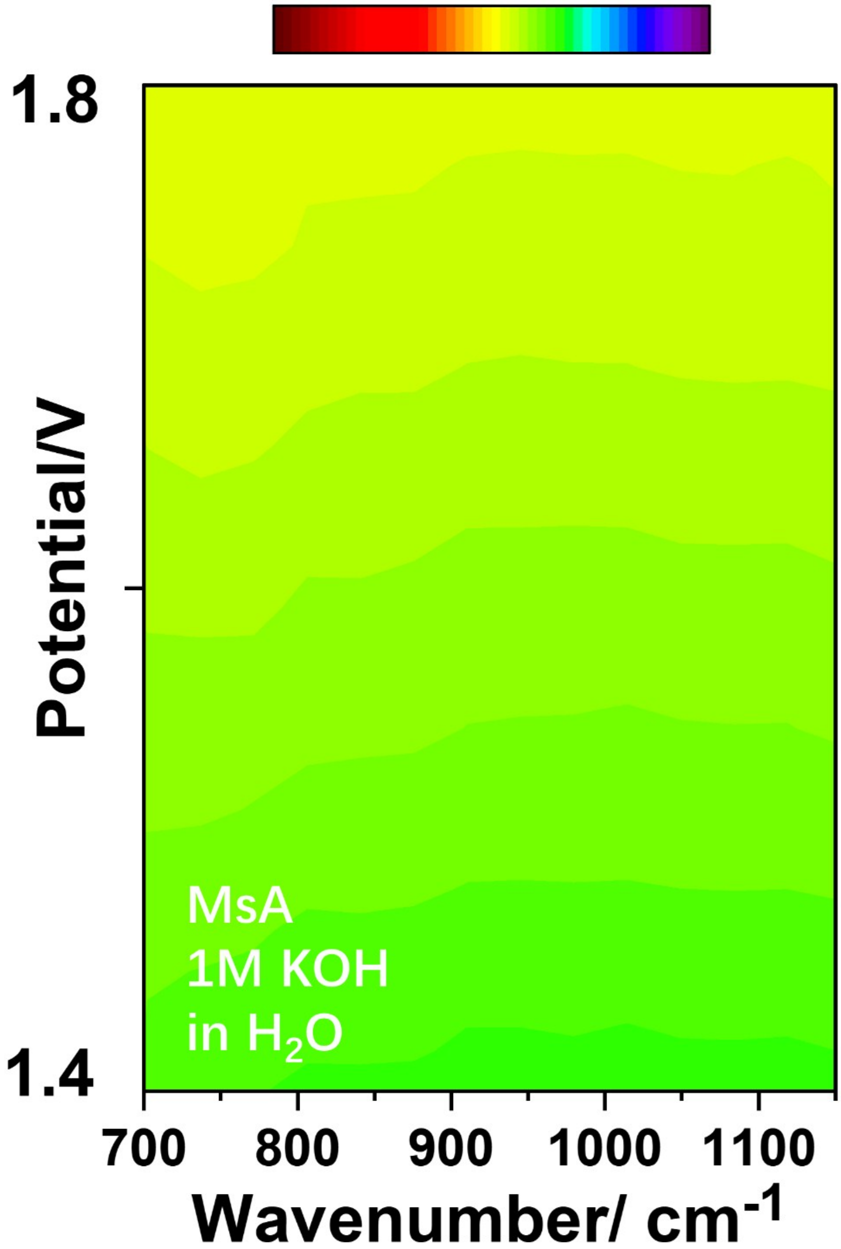

Fig. S12. 2D contour image of operando ATR FT-IR spectrum for MsA electrocatalyst in 1 M KOH in H_2O at the potential range from 1.4 to 1.8 V vs RHE.

Table S1. ICP-AES results of MsA and DmsA.

Sample name	Element	Concentrate （mg/L）
MsA	Ni	15.23
	Fe	5.042
	Cu	4.805
DMsA	Ni	72.69
	Fe	17.11
	Cu	13.13

Table S2. OER performance comparison with recently reported results

Electrocatalysts	Current density (mA cm^{-2})	Corresponding Overpotential (mV)	Tafel slope (mV dec^{-1})	Cycling performance	Reference
DMsA	10	~170	34	200 h at 100 mA cm^{-2}	This work
	100	250			
S|NiNx-PC/EG [1]	10	280	45	10 h at 100 mA cm^{-2}	*Nat. Commun.* 2019, **10**,1392.
	100	330			
G-FeCoW [2]	10	191	—	500 h at 30 mA cm^{-2}	*Science* 2016, **352**,333-337
	100	—			
Fe-ultrathin TiO_2 nanobelt (Fe-UTN) [3]	10	270	37	10 h at 10 mA cm^{-2}	*Angew. Chem. Int. Ed.* 2019, **56**, 2313–2317.
	100	376			
$Co_{1.5}Fe_{0.5}P$ [4]	10	278	57	10 h at 10 mA cm^{-2}	*Angew. Chem. Int. Ed.* 2020, **59**, 465-470.
	100	330			
CoBDC-NF [5]	10	178	51	80 h at 100 mA cm^{-2}	*Nat. Commun.* 2019, **10**,50348.
	100	241			
W-$Ni(OH)_2$ [6]	10	237	33	3 h from 50 to 100 mA cm^{-2}	*Nat. Commun.* 2019, **10**,2149.
	100	~280			
$Co_3Sn_2S_2$ sp(single particle) [7]	10	270	74	12 h at 10 mA cm^{-2}	*Sci. Adv.* 2019, **5**, eaaw9867.
	100	~390			
amorphous LaNiFe hydroxide (a-LNF(t-d)) [8]	10	189	36	100 h at 10 mA cm^{-2}	*Adv. Mater.* 2019, **31**, 1900883.
	100	310			
FeOOH (Se)/IF [9]	10	287	54	14 h at 10 mA cm^{-2}	*J. Am. Chem. Soc.* 2019, **141**, 7005–7013.
	100	364			
NiFe-LDH@NiCu [10]	10	218	57	6 h at 320 mV (~45 mA cm^{-2})	*Adv. Mater.* 2019, **31**, 1806769.
	80	~370			
AN-CuNiFe [11]	10	224	44	12 h at 10 mA cm^{-2}	*Angew. Chem. Int. Ed.* 2019, **131**, 4233–4238.
	50	330			

References:

1 Y. Hou, M. Qiu, M. G. Kim, P. Liu, G. Nam, T. Zhang, X. Zhuang, B. Yang, J. Cho, M. Chen, C. Yuan, L. Lei and X. Feng, *Nat. Commun.*, 2019, **10**, 1392.

2 B. Zhang, X. Zheng, O. Voznyy, R. Comin, M. Bajdich, M. García-Melchor, L. Han, J. Xu, M. Liu, L. Zheng, F. P. García de Arquer, C. T. Dinh, F. Fan, M. Yuan, E. Yassitepe, N. Chen, T. Regier, P. Liu, Y. Li, P. de Luna, A. Janmohamed, H. L. Xin, H. Yang, A. Vojvodic and E. H. Sargent, *Science*, 2016, **352**, 333–337.

3 G. Shen, R. Zhang, L. Pan, F. Hou, Y. Zhao, Z. Shen, W. Mi, C. Shi, Q. Wang, X. Zhang and J.-J. Zou, *Angew. Chem. Int. Ed.*, 2019, **56**, 2313–2317.

4 S. Yang, G. Chen, A. G. Ricciardulli, P. Zhang, Z. Zhang, H. Shi, J. Ma, J. Zhang, P. W. M. Blom and X. Feng, *Angew. Chem. Int. Ed.*, 2020, **59**, 465–470.

5 Z. Xue, K. Liu, Q. Liu, Y. Li, M. Li, C.-Y. Su, N. Ogiwara, H. Kobayashi, H. Kitagawa, M. Liu and G. Li, *Nat. Commun.*, 2019, **10**, 5048.

6 J. Yan, L. Kong, Y. Ji, J. White, Y. Li, J. Zhang, P. An, S. Liu, S.-T. Lee and T. Ma, *Nat. Commun.*, 2019, **10**, 2149.

7 G. Li, Q. Xu, W. Shi, C. Fu, L. Jiao, M. E. Kamminga, M. Yu, H. Tüysüz, N. Kumar, V. Süß, R. Saha, A. K. Srivastava, S. Wirth, G. Auffermann, J. Gooth, S. Parkin, Y. Sun, E. Liu and C. Felser, *Sci. Adv.*, 2019, **5**, eaaw9867.

8 G. Chen, Y. Zhu, H. M. Chen, Z. Hu, S.-F. Hung, N. Ma, J. Dai, H.-J. Lin, C.-T. Chen, W. Zhou and Z. Shao, *Adv. Mater.*, 2019, **31**, 1900883.

9 S. Niu, W.-J. Jiang, Z. Wei, T. Tang, J. Ma, J.-S. Hu and L.-J. Wan, *J. Am. Chem. Soc.*, 2019, **141**, 7005–7013.

10 Y. Zhou, Z. Wang, Z. Pan, Le Liu, J. Xi, X. Luo and Y. Shen, *Adv. Mater.*, 2019, **31**, 1806769.

11 Z. Cai, L. Li, Y. Zhang, Z. Yang, J. Yang, Y. Guo and L. Guo, *Angew. Chem. Int. Ed.*, 2019, **131**, 4233–4238.